

Review

Ionizing Spotlight of Active Galactic Nucleus

Alexei V. Moiseev *  and Aleksandrina A. Smirnova

Special Astrophysical Observatory, Russian Academy of Sciences, 369167 Nizhny Arkhyz, Russia;
ssmirnova@gmail.com

* Correspondence: moisav@sao.ru

Abstract: Ionization cones and relativistic jets give us one of the most large-scale example of active galactic nuclei (AGN) influence on the surrounding gas environment in galaxies and beyond. The study of ionization cones makes it possible not only to test the predictions of the unified model of galactic activity, but also to probe galaxy gas environment and trace how the luminosity of the nucleus changes over time (a light echo). In the external galactic or even extragalactic gas ionization cones create Extended Emission-Line Regions (EELRs) which can span distances from several to hundreds kpc away a host galaxy. We review the recent results of studying the gas kinematics and its ionization properties in EELRs with a special attention to search of fading AGN radiation on the time scale few $\times (10^4 - 10^5)$ years. The role of modern narrow-band and integral-field surveys in these researches is also considered.

Keywords: galaxies: active; galaxies: jets; galaxies: Seyfert; interstellar medium (ISM); nebulae

1. Introduction

There is no doubt that the phenomenon of active galaxy nucleus (AGN) is caused by the accretion of the surrounding matter to the central super massive black hole (SMBH). Until recently, there were only indirect evidences, but now we have images of black holes in the nucleus of the active galaxy M87 [1] and in the Milky Way [2], obtained by radio interferometry. Figure 1 shows the unified model of the ‘accretion engine’ of the AGN [3,4], including a rotating accretion disk of the matter captured by the central black hole, relativistic jet and a gas-dust optically thick torus surrounding the accretion disk. The variety of observed AGN types can be explained by the different orientation of the AGN central engine toward the observer, so that the dust torus hides the accretion disk and the ionized gas clouds closest to the nucleus ($r < 1$ pc) in different ways. These clouds, moving at speeds up to several tens of thousands km s^{-1} , are responsible for the formation of broad components in the lines of ionized hydrogen in the spectra of type 1 Seyfert galaxy (broad line region—BLR). If BLR region is covered from us by a torus, the spectrum of type 2 Seyfert galaxy is directly observed. It contains relatively narrow both recombination and forbidden lines produced by gas clouds at larger distances from SMBH (narrow line region—NLR). The line-of-sight velocities do not exceed several hundreds of km s^{-1} , the size of a typical NLR region ranges from a few hundred parsecs to a few kpc.

The growth and activity of the SMBH is closely related to the host galaxy properties and evolution. The galaxies interaction and secular evolution [5] leads to the loss of angular momentum of the external gas feeding the accretion engine. On the other hand, the active nucleus also demonstrates a noticeable influence on the surrounding interstellar medium and even intergalactic environment. Gas in accretion disk is heated up to high temperatures and radiates both as in the UV as in X-rays. Therefore, we distinguish between mechanical effects (an injection of the kinetic energy of a jet and/or hot winds to the environment) and radiative ones, associated with both ionization of the interstellar medium by energetic quanta, and with the radiation pressure from the accretion engine. Such effect can stop star formation in the galactic gas by ionizing it and heating it up to high temperatures, so that



Citation: Moiseev, A.V.; Smirnova, A.A. Ionizing Spotlight of Active Galactic Nucleus. *Galaxies* **2023**, *11*, 118. <https://doi.org/10.3390/galaxies11060118>

Academic Editor: Luigina Feretti

Received: 12 October 2023

Revised: 1 December 2023

Accepted: 2 December 2023

Published: 7 December 2023



Copyright: © 2023 by the authors. Licensee MDPI, Basel, Switzerland. This article is an open access article distributed under the terms and conditions of the Creative Commons Attribution (CC BY) license (<https://creativecommons.org/licenses/by/4.0/>).

not only fragmentation, but also the existence of cold molecular clouds becomes impossible (negative feedback). On the other hand, the wind from outflow and shock waves associated with jet may compress the gas and trigger the star formation (positive feedback). This symbiosis between the AGN and the parent galaxy makes the activity of the nuclei an important factor in cosmological evolution [6–8].

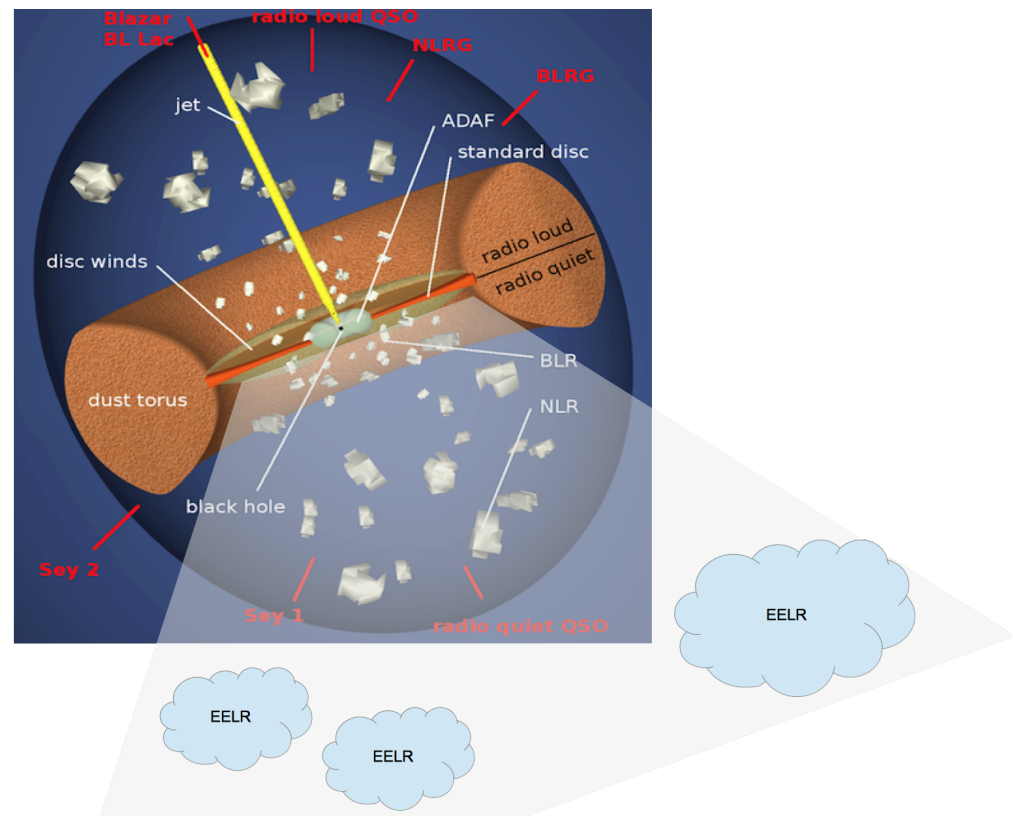


Figure 1. The AGN unified model according Brinkmann [9]. The bottom part (the case of radio-quiet AGNs) shows the ionization cone illuminated the external gas clouds (EELRs).

The dust torus collimates the UV radiation along the disk axis in the form of two symmetric ionization cones [10]. In this way, apart from the BLR and NLR the ‘ionization trace’ of the active nucleus may also be observed at much larger distances from the galaxy center, depending on the presence of neutral gas both in the galactic disk itself and outside it. In the case of gas-rich disk a classical biconical morphology in emission lines distribution will be appeared (the traditional indicator—the doublet of $[O III]\lambda\lambda 4959, 5007$). Otherwise, individual gas clouds can be ionized both inside and outside the galactic disk (see the cone in Figure 1). The typical spatial scale can reaches tens of kpc. Earlier, for such clouds the term ENLR (Extended NLR) was used, but now we considered more general case, including also turbulent gas ejected from the nucleus—EELR (Extended emission line region, [11,12]).

The operation of the accretion engine differs in radio-loud and radio-quiet AGN. In the first case (the upper section of the scheme in Figure 1) most of the energy goes away to the acceleration of relativistic jets particles with the subsequent emission of synchrotron radiation—advection dominated accretion flows (ADAF). In radio-quiet AGN, the contribution of the jets to the total luminosity is insignificant because the most of produced radiation is associated with the accretion disk. This is characteristic of number of quasars, as well as Seyfert and LINER galaxies. These objects make up the vast majority among nearby active galaxies and are the subject of this review.

The ionized cone could be considered as an ‘ionization searchlight’ that illuminates (ionizes) a spatial screen—gas clouds. The study of such systems allows us to better

understand the properties as the searchlight as the screen. We highlight the following main tasks:

- Study of the gas environment of galaxies (accretion of gas clouds, cosmological filaments, etc.)
- ‘Archeology of active galactic nuclei’ [13]—a history of supermassive black hole activity at the light-travel time from the AGN to the gas clouds.
- Constrain of the unified model parameters related with the ionization cones: measuring the cone angle, looking for traces of their precession, constraints of absorbing matter distribution models.

Below we will consider examples of solutions to each of the listed problems, including observations performed by us and our colleagues at the Special Astrophysical Observatory of the Russian Academy of Sciences (SAO RAS) and at the Caucasus Mountain Observatory of the Sternberg Astronomical Institute of the Lomonosov Moscow State University (CMO SAI MSU).

2. Filaments of the Intergalactic Medium

2.1. The Nearest Example: Mrk 6

The lenticular Seyfert galaxy Mrk 6 reveals one of the most nearest and impressive cases of the intergalactic environment illumination by the AGN. Mrk 6—one of the first known Seyfert galaxies, so it seems to have been studied in great detail [14,15]: its stellar disk looks homogeneous and symmetrical. It was also known about large (up to 22 kpc) ionization cone, aligned with the central radio jet [16]. However deep 3D-spectroscopic observations at the SAO RAS 6m telescope with the scanning Fabry-Perot interferometer (https://www.sao.ru/hq/lsvfo/devices/scorpio-2/ifp_eng.html, accessed on 1 December 2023) revealed a very extended system of emission filaments up to distances about 40 kpc (over 4 optical radii) from the nucleus (Figure 2). The velocity field in the H α emission line shows that in the inner regions the rotation of ionized gas takes place in the plane of the stellar disk. The differences in the radial velocities of the gas from the circular rotation model here do not exceed 50 km s⁻¹, but outside the stellar disk the residual velocities reach 250 km s⁻¹. The gas is dynamically cold, i.e., it has a low velocity dispersion ($\sigma < 50$ km s⁻¹) and cannot be associated with jet-driven outflow [17].

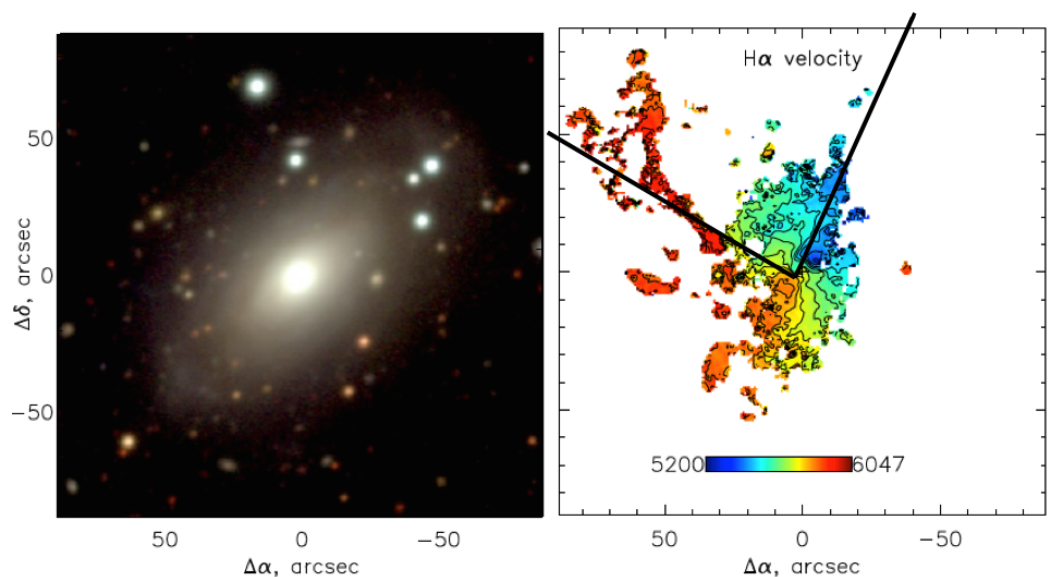


Figure 2. Observations of Mrk 6 at the SAO RAS 6m telescope: the direct image in broad band filters (**left**) and the H α velocity field (**right**) according Smirnova et al. [17]. Black lines mark the ionization cone’s borders according previous estimations in Kukula et al. [16].

In the paper Smirnova et al. [17] we explained the line-of-sight velocity distribution by assuming that the gas in the outer emission structures rotates in circular orbits, approximately perpendicular to the host galaxy disk. The long-slit spectra of the external gas obtained at the 6m telescope demonstrated the ionization by AGN similar with the inner regions of the galaxy. All available data can be explained in the assumption of ionization by AGN radiation of the gas accreted by Mrk 6 from the intergalactic environment. Deep images in broad filters indicate the absence of any stellar structures associated with this gas (tidal tails, disrupted remnants of companions, etc.). It is possible that in the ionized gas we detected part of a much larger H I diffuse structure. The process of external gas accretion is considered as an important stage of galactic baryonic mass assembly (see [18] for review).

2.2. Cosmological Filaments

The accretion of a cold gas from large-scale structure filaments is necessary to form galaxy disk in the frameworks of the Λ CDM cosmology, because it is a way to form disk with a realistic angular momentum (see [19] for review). Therefore the search for fossil traces of this process in the Local Universe is actual. However detailed mapping of neutral hydrogen at high redshifts by modern telescopes is still difficult. Indeed, at redshifts $z > 4$ the 21 cm line shifts to the meter wavelength, so the angular resolution decreases dramatically. However the filaments inside ionization cone can be studied in the optical range. A characteristic example is the detection of a gas filament emitting in the Ly α line, about 290 kpc in size, near the quasar at $z = 2.3$ [20]. In recent years, more and more interesting results in the study of the large-scale gas distribution at $z \approx 3$ have been obtained using the MUSE/VLT integral-field spectrograph (for example, [21,22]). At this redshift the Ly α resonance line falls into the optical range. Results for more distant gas structures in the ionization cones of the Early Univers AGN should be expected in the observations of James Webb Space Telescope (Section 6).

3. Galaxies with Fading Activity

3.1. Duty Cycle of AGN

The well-known tight relations between mass of SMBH and properties of its host galaxy (total mass of the spherical component, galaxy luminosity, etc. [7,23,24]) implies that the most disk and elliptical galaxies harbor a sufficiently massive black hole. However we observe the AGN phenomenon only in a small fraction of galaxies. From the simplest statistical considerations it's clear that duty cycle of activity is a relatively short phase of the galactic nucleus life. Indeed, galactic disk matter needs to lost its angular moment significantly (in $\sim 10^4$ times, according [25]) to move from radius of a few kpc to the nuclear region for consumption by a SMBH. On the one hand, we know a number of processes leading to the angular momentum lost and transfer a matter from several kpc to hundred pc radii orbits: tidal interactions, bars, circumnuclear spirals, binary SMBHs, etc. [25,26]. On the other hand, it is often unclear what feeding mechanism is released in every galaxy, because the timescale of AGN duty cycle differs from characteristic dynamical time of large-scale processes like a galactic merging. The observational information about angular momentum transfer inside inner 10-50 pc is also insufficient, however new ALMA observations shed some light in the case of some nearby Seyfert galaxies [27]. Moreover, the negative feedback effects caused by AGN radiation and/or outflow can terminate the processes of gas inflow. The duration of the active phase and its recurrence is the subject of an intense discussion [13]. Therefore, it is important and interesting to catch the galactic nucleus at the moment when the accretion machine is switch on/off.

Spectral monitoring of nearby AGN and wide-field spectral surveys have revealed a population of galaxies where broad emission lines suddenly appeared or, conversely, completely disappeared (CL-AGN—Changing look AGN). Such event may indicate a change in the geometry of the dusty region or in the accretion rate or some additional effects or their combination ([28–31], see also Ilić et al. in this proceeding). However, the CL-phenomenon is observed on timescales of several years and couldn't be connected

with a global activity trend. On the other hand, it is possible to detect relic extended spatial structures related with previous episode of on-going activity. Low frequency radio observations reveal an example of giant (320 kpc in a projected linear size) diffuse low surface brightness source B2 0924+30 around elliptical galaxy which activity ceased ~ 50 Myr ago [32]. The images of some radio galaxies exhibit possible signatures of two or even three events of activity, like in B0925+420 with a three pairs of radio lobes with ages 0.4–270 Myr [33] or in J1225+4011 with a similar structures correspond to ages 2, 19, and 220 Myr [34]. The current progress in the study of relic structures around radio-loud AGN related with development of modern low-frequency telescopes like LOFAR was recently reviewed by Mahatma [35]. In optical domain a study of the nucleus ionization trace in the surrounding gas allows us to detect AGNs faded at the characteristic time scale ~ 0.1 Myr as it considered below.

3.2. Hanny's Voorwerp

The prototype of the discussed class of objects is Hanny's Voorwerp (translated from Dutch—'Hanny's Object')—a nebula discovered by the volunteer of the Galaxy Zoo citizen project [36] Hanny van Arkel on SDSS images at the projected distance 15–30 kpc from the spiral galaxy IC 2497 (Figure 3, see also [37]). The follow-up spectroscopic observations found that the nebula is an objects at the same redshift with IC 2497 and its spectrum contains strong forbidden lines [O III], [N II], [S II] typical for Seyfert galaxies. The relatively bright lines of helium and neon indicate a high electron temperature—at least 10,000–20,000 K, which could provide either illumination by the AGN or shock waves with velocities $\sim 400 \text{ km s}^{-1}$, what doesn't match to the observed gas kinematics. Meanwhile, the spectrum of the host galaxy indicates only a central star-formation burst and weak LINER-type activity. The observed luminosity in the infrared range is inconsistent with the assumption of a powerful AGN hidden by dust clouds. It was reasonable to assume that the luminosity of the ionizing source had been dramatically decreased by almost two orders of magnitude over the last hundred thousand years [38]. The layout in Figure 3 (based on [12]) explains why we received information about the ionization of the nebula with a delay relative to the photons coming directly from the nucleus.

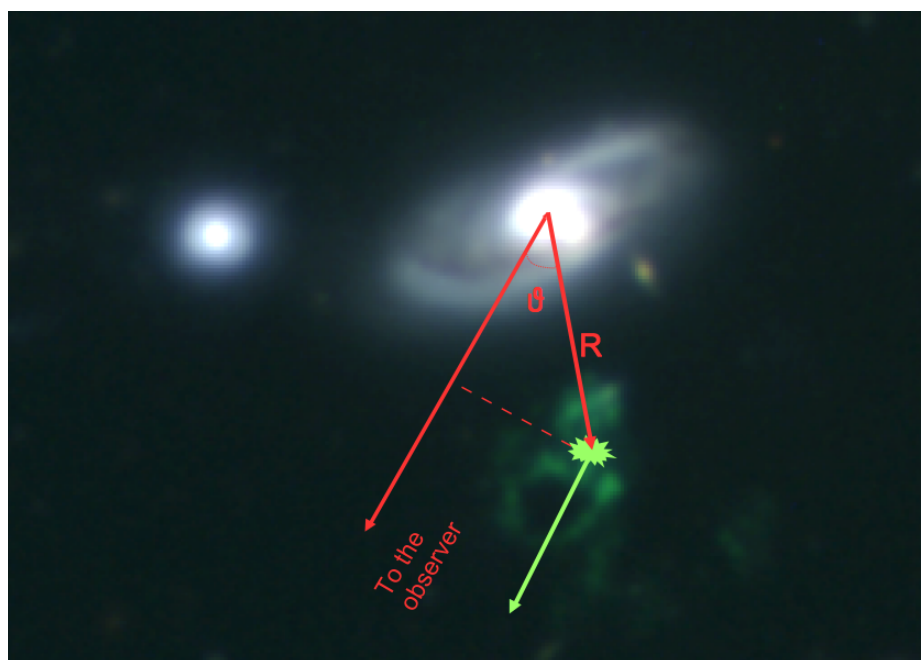


Figure 3. Optical image of the galaxy IC 2497 with its companion and the Hanny's Voorwerp nebula (in green) obtained by the authors at the 6 m telescope in *BVR* filters in October 2011. A geometric scheme illustrating the Equation (1) for the signal delay from the nucleus is overlapping.

The general scenario of the Hanny's Voorwerp (HV) origin (See the illustration in <https://esahubble.org/images/heic1102c/>, accessed on 1 December 2023) looks as follows. Gravitational interaction with a satellite leads both to the formation of a tidal tail emerging from the disk of the host galaxy, and to the inflow gas motions into the disk that started feeding SMBH and as, a consequence, triggered AGN. The nebula appears in emission lines because the gas in the tidal tail getting into the ionization cone. When the gas in the circumnuclear region have been depleted, the relaxation stage occurred and ionization radiation was switched off, but the nebula is still visible for some time for the observer.

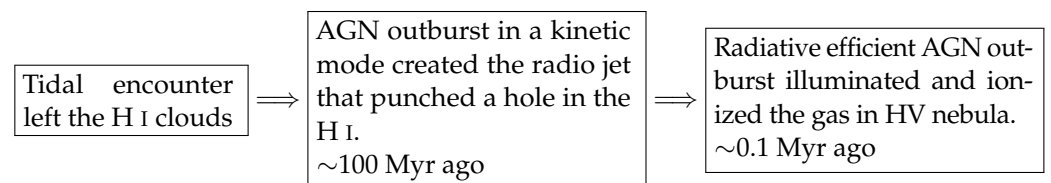
From the diagram shown in Figure 3, the signal delay of the nuclear activity changing is (see [12]):

$$\Delta t = R(1 - \cos \theta) / c = \frac{r_{obs}(1 - \cos \theta)}{c \sin \theta}, \quad (1)$$

where R is the true distance from the nebula to the nucleus, r_{obs} is the observed projection distance, θ is the angle between the directions to the nebula and to the observer.

Since θ is usually unknown, in the papers cited below usually assumed $\Delta t \approx r_{obs}/c$, corresponding to $\theta = 90^\circ$. However, as it follows from the Equation (1), true value Δt may be very different from this rough estimation in the case of other arrangement of the AGN and nebula relative to the observer.

H I mapping has confirmed the existence near the IC 2497 the tail-like structure seen in the neutral hydrogen. At the same time, there is a deficit of H I in the region of the HV ionizing nebula, most likely caused not only by ionizing radiation, but also related with a radio jet kinetic action on the gas [39]. Recent detailed study of the radio jet properties with the LOFAR low frequency radio telescope gives an estimation of its age ~ 100 Myr [40]. The authors of cited work proposed the following scenario of HV evolution that is more complex than described above:



In other words, we observe the signatures of both radio-quiet and radio-loud accretion modes acted during different epoch in the same galaxy.

The gravitationally perturbed systems with HV phenomenon provide a potential opportunity to calculate a duration of AGN duty cycle as a difference between the time when the radiation outburst started and when the activity stopped according Equation (1). Indeed, it's possible to estimate the age of interaction in the merging pair of galaxies using comparison of observed morphological properties and velocity distribution (velocity field) with results of numerical simulations (the GalMer database is an example of such library of 'snapshots' of galactic collision simulations [41]). In this case it becomes possible to understand the mutual spatial orientation of the different components (galaxy disk, tidal tails, ionizing nebula) and also recognize the moment of AGN triggering by gas inflow motions related with tidal forces.

Unfortunately, in the case of IC 2497 there is not enough observational information for this sort of modeling: stellar tidal structures are absent on the available deep images, whereas the presented H I map has too low spatial resolution. There are even doubts that the satellite observed to the east of the main galaxy (Figure 3) is the intruder of the main galaxy structure. Its luminosity and mass seems to be too low for strong tidal disturbance. Therefore, it is important to look for more convenient systems for modeling its spatial structures. Moreover, analysis of the occurrence of HV phenomenon in different sample of galaxies can help us to better understand the character of AGN variability at the timescale 10^4 – 10^5 years from simple statistical considerations (see Section 4).

3.3. New Examples: ‘Voorwerpjes’

How unique is the Hanny’s Voorwerp? The first significant attempt to answer this question was made by Keel et al. [12] in the survey based on the visual examination of SDSS images by participants of the Galaxy Zoo project. They compiled a sample of all nearby ($z < 0.1$) galaxies from SDSS DR7 that were either already in the AGN catalogs or whose line ratio in the SDSS spectra corresponded to possible nuclear activity—a total of 18,116 objects. A close look at the SDSS images revealed 49 candidates with suspected external emission clouds. Follow-up spectroscopy at the 2.1 m Kitt Peak National Observatory and 3 m Lick Observatory telescopes confirmed EELR ionized by AGN in 19 galaxies. It is noteworthy that all systems are either clearly interacting (at least 14/19 according [12]) or are surrounded by faint tidal structures [42]. This fact gives independent agreement with the Hanny’s Voorwerp formation scenario described in the previous section, i.e., that extended ionized gas rises from tidal off-plane structures.

An energetic budget of EELRs was estimated via comparison of the total luminosity of the nucleus in the far infrared range, including the contribution from the heated dust (L_{FIR}), with the luminosity required for ionization of the detected clouds (L_{ion}) [42]. It was found $L_{ion}/L_{FIR} > 1$ for 7 of 20 galaxies (including the prototype—IC 2497) that indicates a fading activity. The remaining objects in the sample could be considered as AGN with obscured nuclear UV radiation.

To apply the scenario of the Hanny’s Voorwerp formation for the new findings (these were called ‘voorwerpjes’ [43]) we have to be sure that the detected gaseous clouds are dynamically quiet. An alternative explanation of EELRs assumes the gas ejected from nuclear region as a result of AGN-driven outflows well known in radio-load quasars [44–46]. The size of EELR related with such outflows can reach several tens of kpc [47,48]. Also jet-cloud interaction leads to the strong shock waves producing the emission line ratio similar with the expected for the ionization cones described above: an excitation of [O III], [S II], and [N II] forbidden lines together with He II $\lambda 4686$ emission (the last one, if the shock exceeds $400\text{--}500\text{ km s}^{-1}$, [12]).

A detailed investigation of the gas kinematics, i.e., distribution of line-of-sight velocity and velocity dispersion, allows to distinguish these two types of EELR (ionization cone vs AGN outflow). This work was made for the fading AGN candidates in the sample from [12] using 3D spectroscopy with the scanning FPI at the 6 m telescope and GMOS integral-field spectrograph [42,49]. It was shown, that ionized gas in the circumnuclear regions ($r < 1\text{--}2\text{ kpc}$) is usually perturbed: it has significant non-circular motions, the velocity dispersion in the [O III] is also large ($\sigma \approx 100\text{--}200\text{ km s}^{-1}$), the emission line profile often has a multicomponent structure. These kinematic features indicate the dynamic effect of the AGN jet and/or wind outflow at the surrounding gas. At the same time, at larger distances from the nucleus, the EELR gas is dynamically cold ($\sigma \approx 10\text{--}50\text{ km s}^{-1}$), the velocity field follows a regular rotation. Moreover, as in the outer filaments of Mrk 6 considered in Section 2.1, the circular rotation does not imply motion in the plane of the host galaxy stellar disk.

The linear size of ionized gas structures in some voorwerpjes exceeds significantly their hosts size. For instance, the nuclear radiation in Teacup (SDSSJ 1430+1339) was traced in the surrounding gaseous nebulae up to projected distance 55 kpc [50,51]. The diameter of EELR in NGC 5972 is about 70 kpc [42].

In many cases the gas illuminated by AGN comes from the external environment with the spin direction different from that of the AGN host. Inclined orbits must precess and fall to the main galactic plane, we can see the complex dust distribution related with shock waves in the warped and precessed gas in galaxies NGC 5972 and SDSS 2201+11 HST images (Figure 4). The corresponded dynamical models are given in [42]. The similar interaction between gas clouds on misalignment orbits appears in some gas-rich polar ring galaxies (see [52], and references therein).

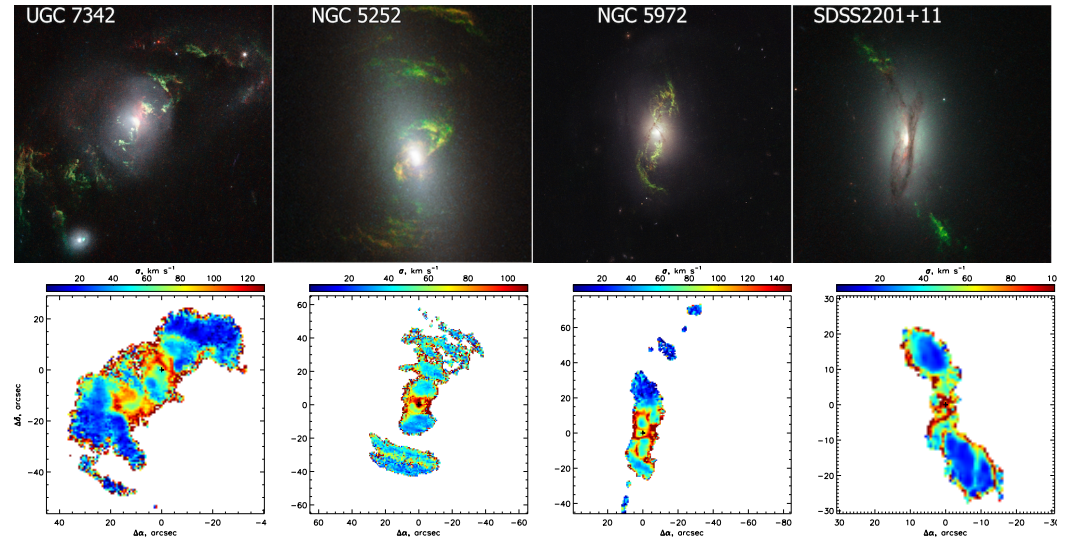


Figure 4. Images of Seyfert galaxies with fading nuclear activity obtained with the HST (top), emission in the [O III] is shown in green (credits: NASA/ESA/W. Keel). The bottom panels show the corresponding maps of the ionized gas velocity dispersion according to the 6m telescope observations [42] (the color scale is in km s^{-1}).

Finally, 3D spectroscopic kinematic mapping gives evidences that ENLRs in found voorwerpjes is ionized by AGN radiation, rather than by shocks. Using the recombination-balance approach to analyse the $H\alpha$ surface brightness of EELR in HST images Keel et al. [49] traced the nuclear ionization history in 8 candidates to the fading AGN selected as described above. It was found that the brightness of regions further from the nucleus corresponds to a higher bolometric luminosity of the nucleus than currently observed. Sometimes these changes are smooth, sometimes its appear rapid drops. But everywhere in the considered sample the luminosity of the central source has been decreasing significantly in the last $\sim 20,000$ years.

The lower limit of the Δt estimation is related with the ionized gas recombination time-scale. The Equation (1) is written for a reflecting nebula, whereas the typical recombination time differs for various combinations of temperature and electron density n_e and can be roughly estimated as [53]:

$$\tau_r \approx (a(\text{ion}, T)n_e)^{-1}, \quad (2)$$

where $a(\text{ion}, T)$ is the total recombination coefficient of the considered ion. According [53] for the ionized hydrogen and $T = 10,000$ K in the usually accepted ‘Case B approximation’: $a(\text{H}^+) = 2.6 \cdot 10^{-13} \text{ cm}^3 \text{ s}^{-1}$. That gives $\tau_r = 1200\text{--}12,000$ years for the density range typical in external EELRs ($n_e = 10 - 100 \text{ cm}^{-3}$ [12,51,54]). It means that in the case of low density gas the observed response in the Balmer emission lines ($H\alpha, H\beta$, etc.) in some considered objects is more smoothed comparing with the pure reflection case in (1). However, high ionized ions recombine significantly faster than H^+ . For instance, the [O III] emission disappears during the time $\tau_r = 20\text{--}200$ years in the same density range for $a(\text{O}^{2+}) = 1.7 \cdot 10^{-11} \text{ cm}^3 \text{ s}^{-1}$ [53,55]. Moreover, in the real plasma the charge exchange reactions make τ_r even shorter for heavy elements ions [56]. It means that the recombination time is not significantly affected the study of EELRs selected according their high [O III]/ $H\beta$ flux ratio (see the Section 4).

4. EELR Statistical Study

4.1. Surveys of Nearby AGNs

The study of individual unique extended ionization cones shades light into the history of AGN triggering and fading of specific galaxies. The smaller and fainter analogue of HV was found in the post-merger galaxy NGC 7252 [57], whereas CFHT and VLT observations of the significantly more distant ($z = 0.326$) galaxy J2240-0927 reveal ENLR ~ 70 kpc in

size [58]. This system of ionized gas clouds has [O III] luminosity on two orders larger than in HV and it is also considered as a result of AGN ionization echo. An EELR with properties resembling other voorwerpjes was found in the post-starburst galaxy PGC 043234 [59] with the MUSE integral-field spectrograph. A very interesting EELR was found in the multi-wavelength study of the interacting pair of galaxies SDSS J1354+1327 [60]. The authors argued that the ~ 10 kpc ionization cone is a result of previous AGN activity, whereas after < 0.1 Myr a new AGN outflow was launched.

The extensive search of EELR candidates by volunteers of the Galaxy Zoo project continues under supervision by Prof. William Keel (University of Alabama) including follow-up snapshot imaging at the HST in the frameworks of Gems of the Galaxy Zoos project [61]. In addition to SDSS, new GalZoo search is based on deeper large-field digital sky surveys like DESI Legacy Imaging Surveys (<https://www.legacysurvey.org/>, accessed on 1 December 2023). A follow-up spectral confirmation of new candidates is carried out at the SAO RAS 6m telescope with SCOPRIO-1/2 multi-mode spectrographs.

The special cases listed above have motivated the search of EELR and the fading AGN phenomenon in samples of galaxies constrained by various criteria in order to minimize the observational bias. 3D spectroscopic data and medium-band filters centered on the doublet [O III] possess a significant advantage over broad-band sky image surveys in the search of a low contrast nebular emission.

The approach based on an integral-field massive survey was recently illustrated by French et al. [54]. The authors gave evidence of 6 EELRs in the sample of 93 post-starburst galaxies selected in Mapping Nearby Galaxies at APO survey (MaNGA [62]). It was shown that 5/6 of found EELRs has ionized by AGN with fading luminosity. The full duty cycle of AGN in post-starburst systems was estimated as ~ 0.1 Myr whereas the luminous phase continues during only about 5% of this time. However the typical radius of these [O III] nebulae does not exceed 10 kpc, that is smaller than in HV and many other systems considered in our review.

The second approach based on the medium-band filters survey is developed in the project TELPERION (Tracking Emission Lines to Probe Extended Regions Ionized by Once-active Nuclei [63,64]). The search of candidates was performed with 1m SARA robotic telescopes with a filter centered on the doublet [O III] $\lambda\lambda 4959, 5007$ for galaxies spanning redshifts $z = 0.009-0.029$. The detection limit of extended emission was about 1/10 of the Hanny's Voorwerp surface brightness.

Strictly speaking, not only ionization cones, but also other type of sources could produce [O III] emission in galaxy outskirts: H II regions, galactic wind outflow driven by central star burst, etc. Optical spectroscopy of selected candidates allows to separate gas clouds with different mechanisms of ionization on the diagnostic diagrams plotting the characteristic flux ratios in the pair of emission lines close in wavelength ([O III]/H β , [N II]/H α , etc.), called 'BPT-diagrams' after the first authors of the paper [65]. Different areas on these diagrams correspond to the gas ionized by UV-radiation of OB-stars in H II-regions, by different types of AGN (UV-radiation in Seyfert galaxies and shocks in LINERs) and by 'composite' ionization between AGN and HII areas (Figure 5). Such diagrams are often supplemented by grids of model calculations of photoionization or shock excitation, taking into account metallicity, shock velocity, magnetic field, etc. [66,67].

Follow-up spectroscopy of the TELPERION, candidates were conducted with several Russian telescopes equipped with high-efficient low-resolution spectrographs developed in SAO RAS under the supervision of Prof. Victor Afanasiev: SCORPIO-1 and SCORPIO-2 prime focal reducers at the SAO RAS 6m telescope spectrograph, ADAM at the 1.6 m telescope AZT33-IK of Sayan Observatory (The description of all listed devices can be found at this URL: https://www.sao.ru/hq/lsvfo/devices_eng.html, accessed on 1 December 2023). For the most interesting confirmed EELRs, deep [O III] images were obtained at the 6m telescope and at the 2.5 m telescope of the SAI MSU using the tunable filter photometer MaNGaL (Mapper of Narrow Galaxy Lines (<https://www.sao.ru/hq/lsvfo/devices/mangal>, accessed on 1 December 2023)). The MaNGaL instrument uses scanning

FPI as a narrow-band filter, about 1.3 nm wide, whose transmission can be fine-tuned to the wavelengths corresponding to both the emission line and the continuum, taking into account the redshift of a target galaxy.

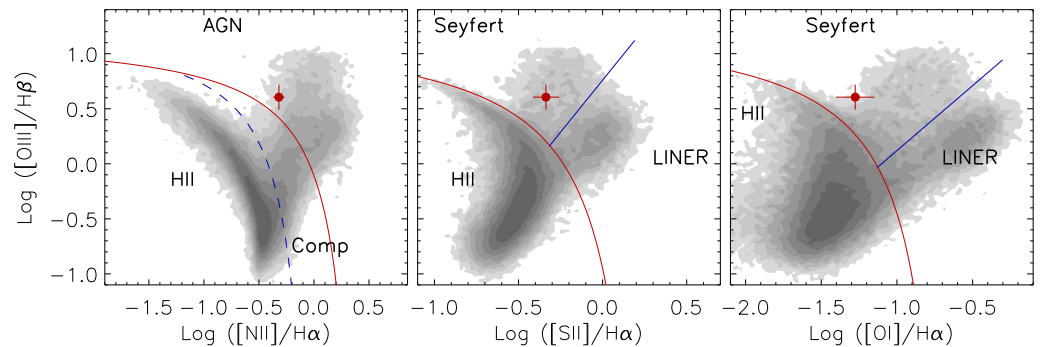


Figure 5. Diagnostic BPT-diagrams from [68], with the flux ratios in the forbidden oxygen, nitrogen, and sulfur lines to the hydrogen Balmer lines. The pairs of lines are close in wavelength, hence the corresponded ratios is not affected by internal extinction. The bounding lines separate the areas corresponding to ionization by young hot stars (HII), the UV continuum of the active nucleus (AGN, Seyfert), and the weak AGN a prominent contribution of shocks (LINER). The positions of galaxy nuclei from the SDSS survey are shown in gray, forming a characteristic ‘seagull diagram’, where the left wing is the sequence of star-forming regions and the right wing is the active galactic nuclei sequence. The red circle with 3σ error bar shows the EELR in NGC 5514 (see the Figure 6).

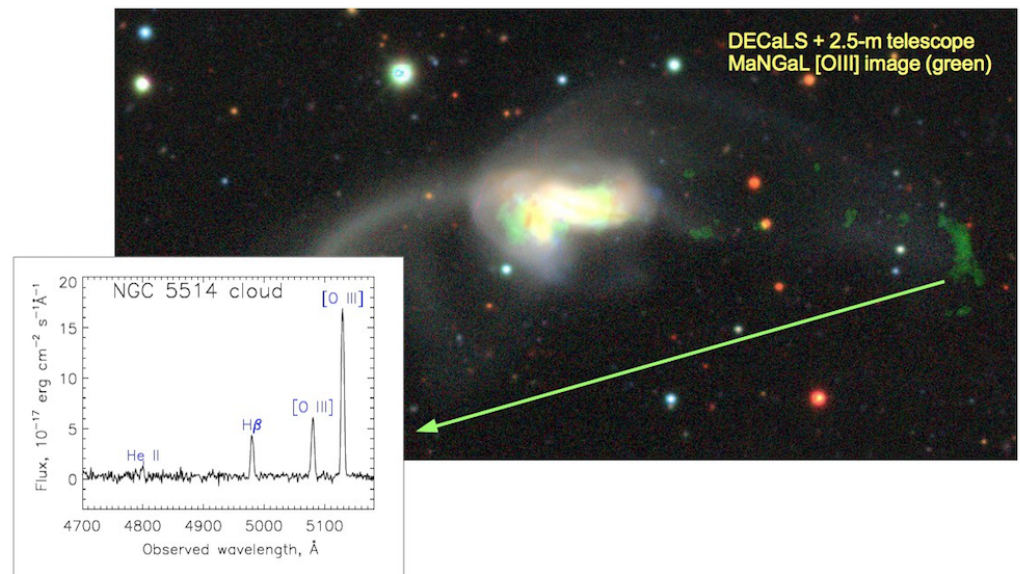


Figure 6. Optical image of the interacting galaxy system NGC 5514 from the DESI Legacy survey [69]. The green color shows the emission distribution in the ionized oxygen line according to the observations with the MaNGaL instrument at the 2.5m SAI MSU telescope. The gas illuminated by the AGN is visible far beyond the disks of galaxies inside the tidal arm. The box shows the spectrum of clouds obtained with the 6m SAO RAS telescope using the SCORPIO-2 instrument. The lines of the ionized oxygen and helium are visible confirming the gas ionization by the active nucleus [64].

With the above technique the first search for distant emission clouds in a luminosity-limited sample of nearby AGN was done [64]. The sample contained 111 galaxies—all known AGN brighter than $M = -20^m$ in the redshift range of $z = 0.009\text{--}0.029$ and $\delta > -36^\circ$. Among 15 emission clouds discovered in [O III] images, 6 gaseous systems were

confirmed as EELRs via follow-up spectroscopy. Two of them (in NGC 235 and NGC 5514) are distant clouds projected at $r = 25 - 75$ kpc from the nucleus.

NGC 5514 (Figure 6) exhibits an almost classical illustration of the described above scenario of the Hanny's Voorwerp formation. In merging pair of galaxies the interaction leads to the gas inflow to the central SMBH in one of the galaxies. The [O III] emission reveals both an inner ionization cone ($r < 12$ kpc) and more distant gas clouds in the tidal tail up to 75 kpc away in projection distance. Whereas in the circumnuclear region signs of AGN-induced outflow is observed, the EELR gas is kinematically quiescent, i.e., it is characterized the low gas velocity dispersion without significant non-circular gas motions. Also the detection He II $\lambda 4861$ emission line (see the spectrum in Figure 6) clearly indicates the ionization by hot source like AGN accretion disk. An alternative explanation is a strong shock excitation, but it the corresponded shock velocities (>400 km s $^{-1}$) disagree with a dynamically cold gas. Also an emission-line ratios indicate the AGN-type photoionization of the distant clouds in NGC 5514 (Figure 5). An estimation of the energetic budget of AGN using the L_{ion}/L_{FIR} criterion shows that activity in NGC 5514 has decreased by more than a factor of 3 in the last ~ 0.25 Myr [64].

In addition to NGC 235 and NGC 5514, large (up to 10 kpc in size) ionization cones inside galactic disks have been found in three galaxies: ESO 362-G08, NGC 7679 (Figure 7) and IC 1481. Interestingly, the latter, as well as NGC 5514, contains a low activity AGN—LINER. Why nucleus with a relatively low ionizing flux produces such prominent cones is not yet very clear. Perhaps this is another indication of the transient activity phenomenon of galactic nuclei in combination with properties of surrounding interstellar medium (gas distribution, its density, metallicity, etc.). Interesting that the prototype voorwerpjes galaxy—IC 2497 (the Hanny's Voorwerp) is also classified as a LINER.

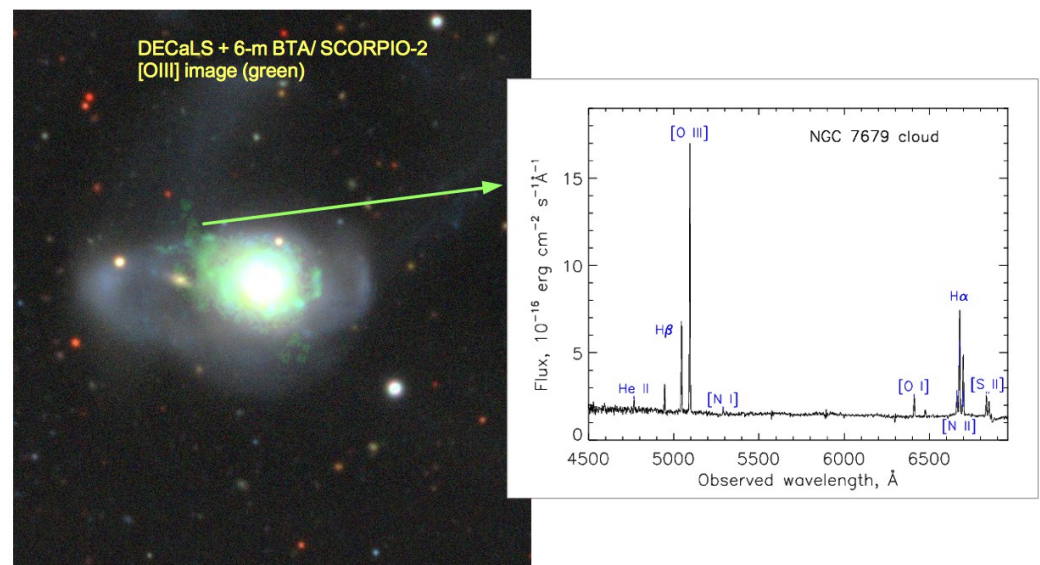


Figure 7. The same as Figure 6 for the galaxy NGC 7679 whereas the [O III] image was conducted with the SCORPIO-2 at the SAO RAS 6m telescope. The AGN illuminates the gas inside the galaxy [64].

Despite the fact that the statistics is not yet very large, the EELRs outside the galaxy stellar disks are detected among 2–5% percent of AGNs depending on selection of samples: bright AGN and Toomre merging sequence [64], AGN with H I external structures [63] or their combinations. Recent counting of the total TELPERION sample of 241 galaxies gives the EELRs incidence $1.7 \pm 0.6\%$ [70]. This fraction in several tens times higher than in the previous Galaxy Zoo survey based on SDSS broad-band images with higher surface brightness threshold. Moreover the EELR detection rate is significantly higher in AGN hosted in interacting and merging galaxies (10–12%, [64,70]). The off-plane gas in tidal

tails enters the cone of illuminating ‘spotlight’ with higher probability and on the larger distances than gas in a galaxy plane.

4.2. Cross-Ionization of a Companion

In all cases discussed above, we learned about a ‘screen’ (a system of gas clouds) because it got inside the AGN ionization. However we can look on the same problem in a different angle: try to determine the radiation cone parameters if the screen geometry is already known.

The first example of known geometry of the screen is a pair where at least one of the companion galaxies contains AGN and the other one is a gas-rich disk galaxy. In this case we can expect cross-ionization effect, when an EELR is created in the companion galaxy’s disk. Such ‘ionizing footprint from a neighbour’s even allow to find hidden AGN in an interacting system, as it was shown in Was 49 [71]. An inverse case is ShaSS 073 in the Shapley supercluster, where the EELR excited in the companion’s disk gave evidences of a dramatic fading of AGN luminosity (in 20 times in the past 30,000 yr) hosted in the second component of the pair at projected separation 21 kpc [72]. The most extreme example of cross-ionization among nearby galaxies was recently found in Mrk 783. The AGN in the main galaxy ionizes not only the surrounding tidal structure up to the distance 41 kpc, but also the external part of the disk of the companion galaxy SDSS J130257.20+162537.1 at the projected distance 99 kpc [73]. The preliminary calculation of the ionized balance indicates that there is no significant decreasing ionizing radiation during last 0.1–0.3 Myr. New in-depth studies of this and similar pairs with integral-field facilities on large telescopes will help to better restore the history of AGN radiation output.

In the close pairs of galaxies it is possible to estimate the solid angle at which the companion disk is visible from the nucleus (see the diagram in Figure 8). Therefore, the width of the ionization cone can be constrained from the statistics of the EELR occurrence in AGN pairs. It was done in the paper [74] considered the sample of pair with Seyfert nucleus in one or both companions selected in the SDSS DR8 according the following criteria: the distance between the nuclei $r < 15''$ (~ 18 kpc for the median redshift $\langle z \rangle = 0.06$), difference in radial velocities within 400 km s^{-1} implies a gravitational bound pairs. Out of 212 pairs, 32 were selected for spectral observations, distinguished by the smallest distance between centers and the largest θ_d angle. Figure 8 shows one of the most interesting system—UGC 6081. The nuclei of both companions are active and two systems of ionization cones are observed simultaneously.

Given the detection rate of cross-ionization occurrence (10/32), the average width of the ionization cone in the sample was evaluated as $\theta_{cone} \approx 70^\circ$ in good agreement with earlier estimations by other methods.

A different value of θ_{cone} was obtained for the other type of a screen with known geometry: in the sample of AGN with extended systems of neutral hydrogen [63] mapped in 21 cm line. From 26 H I-rich systems only one EELR was found. It was the gas clouds projected in 12 kpc away from the nucleus of Seyfert galaxy Mrk 1 that has a common H I envelope with NGC 451 [63]. Calculation gives $\theta_{cone} < 20^\circ$ if the AGN are continuously bright for scales longer than the light-travel times to the external H I structures. The contradiction with previous estimation from cross-ionized pairs is explained if the AGN ionizing radiation undergoes strong variations at times of 10^4 – 10^5 years. This characteristic time is similar that was presented above for fading AGN.

The examples considered in this review are only the first attempts to estimate the characteristics of the AGN accretion machine from the statistics of the occurrence of its ionization trace. Increasing of the samples of such objects as well as more detailed study will make it possible to answer a number of relevant and interesting questions in AGN physics, related, for example, with the precession of the ionization cone or with evolution of dust torus collimating the AGN UV radiation. For this purpose, it is relevant to carry out a deep mapping of the environment of nearby galaxies in the main emission lines (H α , [O III], etc.). Even the first attempts in this direction are already yielding interesting

results. Deep H α imaging of famous nearby interacting pair ‘The Whirlpool’ (NGC 5194/5) revealed an extended low-brightness cloud at 32 kpc away from the center of the main galaxy. The properties of gas excitation correspond to that observed in classical ionization cones [75,76].

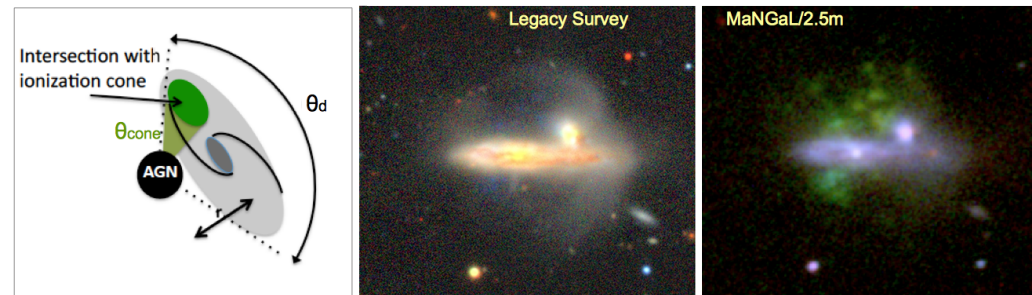


Figure 8. Cross-ionization in galaxy pairs based on [74]. From left to right: the cartoon explaining the geometry of the system consisting of a pair with AGN and nearby spiral galaxy, whose disk is observed from the nucleus at the angle of θ_d ; the image of pair of galaxies UGC 6081 according the DESI Legacy survey; the same field was mapped with the MaNGA instrument on the SAI MSU 2.5 m telescope (emission in the [O III], H α and continuum in the green, red and blue channels correspondently).

It is likely that further study of the Local Group galaxies, will allow to detect new traces of the ionization cones. Accordingly, the question arises: what is about our Milky Way?

5. Activity of the Milky Way Nucleus

Indeed, the SMBH is nesting in the Milky Way nucleus. This fact was confirmed both directly by images [2] and by mass measurements from the kinematics of nearby stars (the Nobel Prize was awarded in 2020 to Reinhard Genzel and Andrea Ghez ‘for the discovery of a supermassive compact object at the centre of our galaxy’). The mass of the SMBH ($4.15 \pm 0.01 \cdot 10^6 M_{\odot}$, [77]) is not very large compared to powerful quasars, but quite sufficient for noticeable manifestations of activity. Such manifestations are known. First of all, its are ‘Fermi bubbles’, named after the Fermi Gamma-ray Space Telescope, which discovered in 2010 two giant spherical structures emitting in the gamma-ray, extending up to ± 10 kpc perpendicular to the galactic plane from the Milky Way center [78]. Formally say, this morphology can also be explained by the galactic wind driven by a circumnuclear burst of star formation. However the required rate of supernovae explosion is much higher than expected. At the same time, the observed specific magnetic field distribution and energy spectrum of cosmic particles of Fermi bubbles are explained in models of recent activity of the Milky Way’s central black hole (Sgr A*), suggesting the age of the bubbles about 2 Myr and a total energy more than 10^{55} erg [79].

The intrigue intensifies when a system of X-ray eROSITA bubbles [80] named after the eROSITA telescope of the Russian-German space observatory ‘Spectrum-Röntgen-Gamma’ was found. These structures of hot gas emitting in the soft X-ray are larger (about 14 kpc) and can be considered as extended envelope of Fermi bubbles. The whole set of observations of both space telescopes can be explained by assuming that it is a single act of energy release in the center of the Galaxy. In this case, the Fermi bubbles correspond to the inner boundary of the most heated interstellar medium, while the eROSITA bubbles correspond to the propagation of the expanding shock wave in the Galactic gaseous halo. The total energy of the process is estimated $\sim 10^{56}$ erg, and the age is 1–2 Myr [80]. Recently a detailed numerical model has been presented suggesting that it was the activity of the Sgr A* jet that formed the observed hot gas bubble system [81].

What is about the ionizing activity of the Milky Way’s nucleus? In addition to the gas in the galactic disk the system of outer clouds is exist, that allows us to detect a possible trace of the ‘ionization spotlight’. It is the Magellanic Stream—a giant arch of neutral

hydrogen stretching almost through the entire southern galactic hemisphere. There is virtually no doubt that this gas is associated with satellites of the Milky Way—the Large and Small Magellanic Clouds. Most likely it's a matter lost by them under the action of the Galaxy gravity. Bland-Hawthorn et al. [82,83] showed that some part of the gas in Magellanic Stream is ionized, with the ionization properties corresponded to the excitation by hard radiation from the Seyfert nucleus.

The axis of the inferred ionization cone deviates only 15° from the Galactic rotation axis, and the width of the cone ($\sim 60^\circ$) agrees well with the estimates given above for such structures in other AGN. The time elapsed since the ionization activity (3.5 ± 0.1 Myr) is quite consistent with the age of the Fermi-eROSITA bubbles, therefore it is likely to be a single act of activity. Any case, new breakthroughs in both observations and numerical simulations should be expected in this field of Galaxy research.

6. Ionization Cones and Nuclear Outflows

Our review is mostly focuses on the search and study of kinematically-quiet EELRs that are in dynamical equilibrium with the host galaxy, which can be considered as one of the best tracer both of the AGN ionization output and low-density intergalactic medium. However, as it was already mentioned in Section 3.3, there is a population of kinematically hot EELRs produces by nuclear outflows driven by jet-cloud interaction or thermal energy and radiation pressure from the accretion disk (see the recent review [84], and references therein). A detailed description of this phenomenon is beyond the scopes of this review, however in many cases we observe a mix of both acts, i.e., kpc-scale outflow ionized by AGN. One of the nearest luminous quasar—the Teacup galaxy ($z = 0.09$) exhibits this kind of composite structure. A well-described ~ 12 kpc ionized gas bubble inflated by the AGN outflow was included in the list of voorwerpjes with ionization balance corresponds to fading AGN [42]. Long-slit spectroscopy at the Gran Telescopio Canarias revealed that this bubble is only internal part of a giant emission nebula ~ 100 kpc in size [50]. The nebula was mapped in the [O III] emission line at the 6 m telescope, it was shown that the external emission arcs might be a remnant of the previous outflow (the age < 0.8 Gyr) ionized by the AGN radiation [51]. Whereas the forthcoming integral-field observations with MUSE at the 8m Very Large Telescope allows to study in details properties of the ionized gas outflow up to 30 kpc from the AGN [85].

Teacup AGN can be considered as a local prototype of combined influence of the AGN radiation and outflow on the surrounding matter on scales of the host galaxy and beyond in the high redshift Universe. These effects were considered in set of cosmological simulations (for instance, [86–88]). It is possible that [C II]-emitted haloes recently discovered in star forming and AGN early galaxies at $z \sim 6$ [89–91] are evolutionary related with local EELRs considered in our review. New space telescope JWST is ushering in a new era of study AGN outflows and ionization cones in 'cosmic noon' period ($z = 1 - 3$) as it was already demonstrated in the first published results [92,93].

7. Conclusions and Future Directions

The authors hope that in this brief review they have been able to show how observations of extended (and distant) emission clouds provide information about the kinematics and state of gas ionization at distances up to tens and even hundreds of kpc from the center of galaxies. The study of the active nucleus ionizing cones makes it possible to trace the processes of low-density cold gas accretion by galaxies with much better angular resolution than in HI to examine the activity history of a supermassive black hole on time scales of 10^4 – 10^5 years, and even to constrain the parameters of the accretion machine hidden inside the central parsec. Moreover, such studies are also relevant in the case of our own Galaxy.

Author Contributions: Conceptualization, A.V.M. and A.A.S.; writing—original draft preparation, A.V.M.; writing—review and editing, A.A.S. All authors have read and agreed to the published version of the manuscript.

Funding: The work was performed as part of the SAO RAS government contract approved by the Ministry of Science and Higher Education of the Russian Federation.

Data Availability Statement: The original data presented in this study are openly available in the General observation data archive of SAO RAS: <https://www.sao.ru/oasis/fetch.html> (accessed on 1 December 2023). The reduced data presented in this study are available on request from the corresponding author.

Acknowledgments: This work is dedicated to the memory of Victor Afanasiev whose developed the spectral instruments for 6 m and 1.6 m telescopes and to the memory of Victor Kornilov whose enthusiasm and knowledge make the 2.5 m telescope work successfully. We thank the reviewers for their constructive comments. Observations with the SAO RAS telescopes are supported by the Ministry of Science and Higher Education of the Russian Federation. The renovation of telescope equipment is currently provided within the national project “Science and Universities”. The Legacy Surveys consist of three individual and complementary projects: the Dark Energy Camera Legacy Survey (DECaLS; Proposal ID #2014B-0404; PIs: David Schlegel and Arjun Dey), the Beijing-Arizona Sky Survey (BASS; NOAO Prop. ID #2015A-0801; PIs: Zhou Xu and Xiaohui Fan), and the Mayall z-band Legacy Survey (MzLS; Prop. ID #2016A-0453; PI: Arjun Dey). DECaLS, BASS, and MzLS together include data obtained, respectively, at the Blanco telescope, Cerro Tololo Inter-American Observatory, NSF’s NOIRLab; the Bok telescope, Steward Observatory, University of Arizona; and the Mayall telescope, Kitt Peak National Observatory, NOIRLab. NOIRLab is operated by the Association of Universities for Research in Astronomy (AURA) under a cooperative agreement with the National Science Foundation. The Legacy Survey team makes use of data products from the Near-Earth Object Wide-field Infrared Survey Explorer (NEOWISE), which is a project of the Jet Propulsion Laboratory/California Institute of Technology. NEOWISE is funded by the National Aeronautics and Space Administration. The Legacy Surveys imaging of the DESI footprint is supported by the Director, Office of Science, Office of High Energy Physics of the U.S. Department of Energy under Contract No. DE-AC02-05CH1123; by the National Energy Research Scientific Computing Center, a DOE Office of Science User Facility under the same contract; and by the U.S. National Science Foundation, Division of Astronomical Sciences under Contract No. AST-0950945 to NOAO.

Conflicts of Interest: The authors declare no conflict of interest.

Abbreviations

The following abbreviations are used in this manuscript:

AGN	Active galaxy nucleus
EELR	Extended Emission-Line Regions
FPI	Fabry-Perot interferometer
JWST	James Webb Space Telescope
HST	Hubble Space Telescope
HV	Hanni’s Voorwerp
LINER	Low-ionization nuclear emission-line region
LOFAR	International Low-Frequency Array
MUSE	Multi Unit Spectroscopic Explorer
SAI MSU	Sternberg Astronomical Institute of Lomonosov Moscow State University
SAO RAS	Special Astrophysical Observatory of the Russian Academy of Sciences
SCORPIO	Spectral Camera with Optical Reducer for Photometric and Interferometric Observations
SDSS	Sloan Digital Sky Survey
Sy	Seyfert galaxy

References

1. Event Horizon Telescope Collaboration; Akiyama, K.; Alberdi, A.; Alef, W.; Asada, K.; Azulay, R.; Bacsko, A.K.; Ball, D.; Baloković, M.; Barrett, J.; et al. First M87 Event Horizon Telescope Results. IV. Imaging the Central Supermassive Black Hole. *Astrophys. J. Lett.* **2019**, *875*, L4. [[CrossRef](#)]
2. Event Horizon Telescope Collaboration; Akiyama, K.; Alberdi, A.; Alef, W.; Algaba, J.C.; Anantua, R.; Asada, K.; Azulay, R.; Bach, U.; Bacsko, A.K.; et al. First Sagittarius A* Event Horizon Telescope Results. I. The Shadow of the Supermassive Black Hole in the Center of the Milky Way. *Astrophys. J. Lett.* **2022**, *930*, L12. [[CrossRef](#)]
3. Antonucci, R. Unified models for active galactic nuclei and quasars. *ARA&A* **1993**, *31*, 473–521. [[CrossRef](#)]

4. Urry, C.M.; Padovani, P. Unified Schemes for Radio-Loud Active Galactic Nuclei. *Publ. Astron. Soc. Pac.* **1995**, *107*, 803. [[CrossRef](#)]
5. Kormendy, J.; Kennicutt, R.C.J. Secular Evolution and the Formation of Pseudobulges in Disk Galaxies. *ARA&A* **2004**, *42*, 603–683. [[CrossRef](#)]
6. Silk, J.; Mamon, G.A. The current status of galaxy formation. *Res. Astron. Astrophys.* **2012**, *12*, 917–946. [[CrossRef](#)]
7. Kormendy, J.; Ho, L.C. Coevolution (Or Not) of Supermassive Black Holes and Host Galaxies. *ARA&A* **2013**, *51*, 511–653. [[CrossRef](#)]
8. Pillepich, A.; Springel, V.; Nelson, D.; Genel, S.; Naiman, J.; Pakmor, R.; Hernquist, L.; Torrey, P.; Vogelsberger, M.; Weinberger, R.; et al. Simulating galaxy formation with the IllustrisTNG model. *Mon. Not. R. Astron. Soc.* **2018**, *473*, 4077–4106. [[CrossRef](#)]
9. Brinkmann, S. On the Numerical Simulation of Advection Dominated Accretion Flows. Ph.D. Thesis, Ruprecht-Karls University of Heidelberg, Heidelberg, Germany, 2009.
10. Wilson, A.S.; Tsvetanov, Z.I. Ionization Cones and Radio Ejecta in Active Galaxies. *Astron. J.* **1994**, *107*, 1227. [[CrossRef](#)]
11. Stockton, A.; Fu, H.; Canalizo, G. QSO extended emission-line regions. *New Astron. Rev.* **2006**, *50*, 694–700. [[CrossRef](#)]
12. Keel, W.C.; Chojnowski, S.D.; Bennert, V.N.; Schawinski, K.; Lintott, C.J.; Lynn, S.; Pancoast, A.; Harris, C.; Nierenberg, A.M.; Sonnenfeld, A.; et al. The Galaxy Zoo survey for giant AGN-ionized clouds: Past and present black hole accretion events. *Mon. Not. R. Astron. Soc.* **2012**, *420*, 878–900. [[CrossRef](#)]
13. Morganti, R. Archaeology of active galaxies across the electromagnetic spectrum. *Nat. Astron.* **2017**, *1*, 596–605. [[CrossRef](#)]
14. Capetti, A.; Axon, D.J.; Kukula, M.; Macchetto, F.; Pedlar, A.; Sparks, W.B.; Boksenberg, A. The Emission-Line Jet in Markarian 6*. *Astrophys. J. Lett.* **1995**, *454*, L85. [[CrossRef](#)]
15. Afanasiev, V.L.; Popović, L.Č.; Shapovalova, A.I.; Borisov, N.V.; Ilić, D. Variability in spectropolarimetric properties of Sy 1.5 galaxy Mrk 6. *Mon. Not. R. Astron. Soc.* **2014**, *440*, 519–529. [[CrossRef](#)]
16. Kukula, M.J.; Holloway, A.J.; Pedlar, A.; Meaburn, J.; Lopez, J.A.; Axon, D.J.; Schilizzi, R.T.; Baum, S.A. Unusual radio and optical structures in the Seyfert galaxy Markarian 6. *Mon. Not. R. Astron. Soc.* **1996**, *280*, 1283–1292. [[CrossRef](#)]
17. Smirnova, A.A.; Moiseev, A.V.; Dodonov, S.N. A close look at the well-known Seyfert galaxy: Extended emission filaments in Mrk 6. *Mon. Not. R. Astron. Soc.* **2018**, *481*, 4542–4547. [[CrossRef](#)]
18. Sánchez Almeida, J.; Elmegreen, B.G.; Muñoz-Tuñón, C.; Elmegreen, D.M. Star formation sustained by gas accretion. *Astron. Astrophys. Rev.* **2014**, *22*, 71. [[CrossRef](#)]
19. Sil’chenko, O.K. Empirical scenarios of galaxy evolution. *Phys. Usp.* **2022**, *65*, 1224–1247. [[CrossRef](#)]
20. Cantalupo, S.; Arrigoni-Battaia, F.; Prochaska, J.X.; Hennawi, J.F.; Madau, P. A cosmic web filament revealed in Lyman- α emission around a luminous high-redshift quasar. *Nature* **2014**, *506*, 63–66. [[CrossRef](#)]
21. Sanderson, K.N.; Prescott, M.K.M.; Christensen, L.; Fynbo, J.; Møller, P. Mapping the Morphology and Kinematics of a Ly α -selected Nebula at $z = 3.15$ with MUSE. *Astrophys. J.* **2021**, *923*, 252. [[CrossRef](#)]
22. Wang, W.; Wylezalek, D.; Vernet, J.; De Breuck, C.; Gullberg, B.; Swinbank, M.; Villar Martín, M.; Lehnert, M.; Drouart, G.; Arrigoni Battaia, F.; et al. 3D tomography of the giant Ly α nebulae of $z \approx 3$ –5 radio-loud AGN. *arXiv* **2023**, arXiv:2309.15144. [[CrossRef](#)]
23. Gebhardt, K.; Bender, R.; Bower, G.; Dressler, A.; Faber, S.M.; Filippenko, A.V.; Green, R.; Grillmair, C.; Ho, L.C.; Kormendy, J.; et al. A Relationship between Nuclear Black Hole Mass and Galaxy Velocity Dispersion. *Astrophys. J. Lett.* **2000**, *539*, L13–L16. [[CrossRef](#)]
24. Ferrarese, L.; Merritt, D. A Fundamental Relation between Supermassive Black Holes and Their Host Galaxies. *Astrophys. J. Lett.* **2000**, *539*, L9–L12. [[CrossRef](#)]
25. Jogee, S. The Fueling and Evolution of AGN: Internal and External Triggers. In *Physics of Active Galactic Nuclei at All Scales*; Alloin, D., Ed.; Springer: Berlin/Heidelberg, Germany, 2006; Volume 693, p. 143. [[CrossRef](#)]
26. Combes, F. Fueling the AGN. In *Advanced Lectures on the Starburst-AGN*; Aretxaga, I., Kunth, D., Mújica, R., Eds.; World Scientific Publishing Company: Singapore, 2001; p. 223. [[CrossRef](#)]
27. Combes, F. Circum-nuclear molecular disks: Role in AGN fueling and feedback. In *Galaxy Evolution and Feedback across Different Environments*; Storchi Bergmann, T., Forman, W., Overzier, R., Riffel, R., Eds.; Cambridge University Press: Cambridge, UK, 2021; Volume 359, pp. 312–317. [[CrossRef](#)]
28. LaMassa, S.M.; Cales, S.; Moran, E.C.; Myers, A.D.; Richards, G.T.; Eracleous, M.; Heckman, T.M.; Gallo, L.; Urry, C.M. The Discovery of the First “Changing Look” Quasar: New Insights Into the Physics and Phenomenology of Active Galactic Nucleus. *Astrophys. J.* **2015**, *800*, 144. [[CrossRef](#)]
29. MacLeod, C.L.; Ross, N.P.; Lawrence, A.; Goad, M.; Horne, K.; Burgett, W.; Chambers, K.C.; Flewelling, H.; Hodapp, K.; Kaiser, N.; et al. A systematic search for changing-look quasars in SDSS. *Mon. Not. R. Astron. Soc.* **2016**, *457*, 389–404. [[CrossRef](#)]
30. Ricci, C.; Trakhtenbrot, B. Changing-look Active Galactic Nuclei. *arXiv* **2022**, arXiv:2211.05132.
31. Popović, L.Č.; Ilić, D.; Burenkov, A.; Patiño Alvarez, V.M.; Marčeta-Mandić, S.; Kovačević-Dojčinović, J.; Shablovinskaya, E.; Kovačević, A.B.; Marziani, P.; Chavushyan, V.; et al. Long-term optical spectral monitoring of a changing-look active galactic nucleus NGC 3516. II. Broad-line profile variability. *Astron. Astrophys.* **2023**, *675*, A178. [[CrossRef](#)]
32. Shulevski, A.; Morganti, R.; Harwood, J.J.; Barthel, P.D.; Jamrozy, M.; Brienza, M.; Brunetti, G.; Röttgering, H.J.A.; Murgia, M.; White, G.J.; et al. Radiative age mapping of the remnant radio galaxy B2 0924+30: The LOFAR perspective. *Astron. Astrophys.* **2017**, *600*, A65. [[CrossRef](#)]

33. Brocksopp, C.; Kaiser, C.R.; Schoenmakers, A.P.; de Bruyn, A.G. Three episodes of jet activity in the Fanaroff-Riley type II radio galaxy B0925+420. *Mon. Not. R. Astron. Soc.* **2007**, *382*, 1019–1028. [[CrossRef](#)]
34. Chavan, K.; Dabhade, P.; Saikia, D.J. A giant radio galaxy with three cycles of episodic jet activity from LoTSS DR2. *Mon. Not. R. Astron. Soc.* **2023**, *525*, L87–L92. [[CrossRef](#)]
35. Mahatma, V.H. The Dynamics and Energetics of Remnant and Restarting RLAGN. *Galaxies* **2023**, *11*, 74. [[CrossRef](#)]
36. Lintott, C.J.; Schawinski, K.; Slosar, A.; Land, K.; Bamford, S.; Thomas, D.; Raddick, M.J.; Nichol, R.C.; Szalay, A.; Andreescu, D.; et al. Galaxy Zoo: Morphologies derived from visual inspection of galaxies from the Sloan Digital Sky Survey. *Mon. Not. R. Astron. Soc.* **2008**, *389*, 1179–1189. [[CrossRef](#)]
37. Keel, W.C.; Lintott, C.J.; Schawinski, K.; Bennert, V.N.; Thomas, D.; Manning, A.; Chojnowski, S.D.; van Arkel, H.; Lynn, S. The History and Environment of a Faded Quasar: Hubble Space Telescope Observations of Hanny’s Voorwerp and IC 2497. *Astron. J.* **2012**, *144*, 66. [[CrossRef](#)]
38. Lintott, C.J.; Schawinski, K.; Keel, W.; van Arkel, H.; Bennert, N.; Edmondson, E.; Thomas, D.; Smith, D.J.B.; Herbert, P.D.; Jarvis, M.J.; et al. Galaxy Zoo: ‘Hanny’s Voorwerp’, a quasar light echo? *Mon. Not. R. Astron. Soc.* **2009**, *399*, 129–140. [[CrossRef](#)]
39. Józsa, G.I.G.; Garrett, M.A.; Oosterloo, T.A.; Rampadarath, H.; Paragi, Z.; van Arkel, H.; Lintott, C.; Keel, W.C.; Schawinski, K.; Edmondson, E. Revealing Hanny’s Voorwerp: Radio observations of IC 2497. *Astron. Astrophys.* **2009**, *500*, L33–L36. [[CrossRef](#)]
40. Smith, D.J.B.; Krause, M.G.; Hardcastle, M.J.; Drake, A.B. Relic jet activity in ‘Hanny’s Voorwerp’ revealed by the LOFAR two metre sky survey. *Mon. Not. R. Astron. Soc.* **2022**, *514*, 3879–3885. [[CrossRef](#)]
41. Chilingarian, I.V.; Di Matteo, P.; Combes, F.; Melchior, A.L.; Semelin, B. The GalMer database: Galaxy mergers in the virtual observatory. *Astron. Astrophys.* **2010**, *518*, A61. [[CrossRef](#)]
42. Keel, W.C.; Maksym, W.P.; Bennert, V.N.; Lintott, C.J.; Chojnowski, S.D.; Moiseev, A.; Smirnova, A.; Schawinski, K.; Urry, C.M.; Evans, D.A.; et al. HST Imaging of Fading AGN Candidates. I. Host-galaxy Properties and Origin of the Extended Gas. *Astron. J.* **2015**, *149*, 155. [[CrossRef](#)]
43. Garrett, M.A. Hanny’s Voorwerp and the Antikythera Mechanism-similarities, differences and insights. In Proceedings of the from Antikythera to the Square Kilometre Array: Lessons from the Ancients, Kerastari, Greece, 12–15 June 2012; p. 47. [[CrossRef](#)]
44. Fu, H.; Stockton, A. Extended Emission-Line Regions: Remnants of Quasar Superwinds? *Astrophys. J.* **2009**, *690*, 953–973. [[CrossRef](#)]
45. Harrison, C.M.; Alexander, D.M.; Mullaney, J.R.; Swinbank, A.M. Kiloparsec-scale outflows are prevalent among luminous AGN: Outflows and feedback in the context of the overall AGN population. *Mon. Not. R. Astron. Soc.* **2014**, *441*, 3306–3347. [[CrossRef](#)]
46. Rupke, D.S.N.; Veilleux, S. Integral Field Spectroscopy of Massive, Kiloparsec-scale Outflows in the Infrared-luminous QSO Mrk 231. *Astrophys. J. Lett.* **2011**, *729*, L27. [[CrossRef](#)]
47. Vayner, A.; Wright, S.A.; Murray, N.; Armus, L.; Boehle, A.; Cosens, M.; Larkin, J.E.; Mieda, E.; Walth, G. A Spatially Resolved Survey of Distant Quasar Host Galaxies. I. Dynamics of Galactic Outflows. *Astrophys. J.* **2021**, *919*, 122. [[CrossRef](#)]
48. Villar Martín, M.; Emonts, B.H.C.; Cabrera Lavers, A.; Bellocchi, E.; Alonso Herrero, A.; Humphrey, A.; Dall’Agnol de Oliveira, B.; Storchi-Bergmann, T. Interactions between large-scale radio structures and gas in a sample of optically selected type 2 quasars. *Astron. Astrophys.* **2021**, *650*, A84. [[CrossRef](#)]
49. Keel, W.C.; Lintott, C.J.; Maksym, W.P.; Bennert, V.N.; Chojnowski, S.D.; Moiseev, A.; Smirnova, A.; Schawinski, K.; Sartori, L.F.; Urry, C.M.; et al. Fading AGN Candidates: AGN Histories and Outflow Signatures. *Astrophys. J.* **2017**, *835*, 256. [[CrossRef](#)]
50. Villar-Martín, M.; Cabrera-Lavers, A.; Humphrey, A.; Silva, M.; Ramos Almeida, C.; Piqueras-López, J.; Emonts, B. A 100 kpc nebula associated with the ‘Teacup’ fading quasar. *Mon. Not. R. Astron. Soc.* **2018**, *474*, 2302–2312. [[CrossRef](#)]
51. Moiseev, A.V.; Ikhsanova, A.I. Gas and Stars in the Teacup Quasar Looking with the 6-m Telescope. *Universe* **2023**, *9*, 66. [[CrossRef](#)]
52. Moiseev, A. Polar Structures in Late-Type Galaxies. In *Multi-Spin Galaxies*; Astronomical Society of the Pacific Conference Series; Iodice, E., Corsini, E.M., Eds.; Astronomical Society of the Pacific: San Francisco, CA, USA, 2014; Volume 486, p. 61. [[CrossRef](#)]
53. Osterbrock, D.E.; Ferland, G.J. *Astrophysics of Gaseous Nebulae and Active Galactic Nuclei*; University Science Books: Herndon, VA, USA, 2006.
54. French, K.D.; Earl, N.; Novack, A.B.; Padasani, B.; Pillai, V.R.; Tripathi, A.; Verrico, M.E. Fading AGNs in Poststarburst Galaxies. *Astrophys. J.* **2023**, *950*, 153. [[CrossRef](#)]
55. Crenshaw, D.M.; Kraemer, S.B.; Schmitt, H.R.; Jaffé, Y.L.; Deo, R.P.; Collins, N.R.; Fischer, T.C. The Geometry of Mass Outflows and Fueling Flows in the Seyfert 2 Galaxy MRK 3. *Astron. J.* **2010**, *139*, 871–877. [[CrossRef](#)]
56. Binette, L.; Robinson, A. Fossil nebulae in the context of active galaxies. I. Time evolution of a single cloud. *Astron. Astrophys.* **1987**, *177*, 11–21.
57. Schweizer, F.; Seitzer, P.; Kelson, D.D.; Villanueva, E.V.; Walth, G.L. The [O III] Nebula of the Merger Remnant NGC 7252: A Likely Faint Ionization Echo. *Astrophys. J.* **2013**, *773*, 148. [[CrossRef](#)]
58. Schirmer, M.; Diaz, R.; Holmberg, K.; Levenson, N.A.; Winge, C. A Sample of Seyfert-2 Galaxies with Ultraluminous Galaxy-wide Narrow-line Regions: Quasar Light Echoes? *Astrophys. J.* **2013**, *763*, 60. [[CrossRef](#)]
59. Prieto, J.L.; Krühler, T.; Anderson, J.P.; Galbany, L.; Kochanek, C.S.; Aquino, E.; Brown, J.S.; Dong, S.; Förster, F.; Holoién, T.W.S.; et al. MUSE Reveals a Recent Merger in the Post-starburst Host Galaxy of the TDE ASASSN-14li. *Astrophys. J. Lett.* **2016**, *830*, L32. [[CrossRef](#)]

60. Comerford, J.M.; Barrows, R.S.; Müller-Sánchez, F.; Nevin, R.; Greene, J.E.; Pooley, D.; Stern, D.; Harrison, F.A. An Active Galactic Nucleus Caught in the Act of Turning Off and On. *Astrophys. J.* **2017**, *849*, 102. [[CrossRef](#)]
61. Keel, W.C.; Tate, J.; Wong, O.I.; Banfield, J.K.; Lintott, C.J.; Masters, K.L.; Simmons, B.D.; Scarlata, C.; Cardamone, C.; Smethurst, R.; et al. Gems of the Galaxy Zoos—A Wide-ranging Hubble Space Telescope Gap-filler Program. *Astron. J.* **2022**, *163*, 150. [[CrossRef](#)]
62. Yan, R.; Tremonti, C.; Bershady, M.A.; Law, D.R.; Schlegel, D.J.; Bundy, K.; Drory, N.; MacDonald, N.; Bizyaev, D.; Blanc, G.A.; et al. SDSS-IV/MaNGA: Spectrophotometric Calibration Technique. *Astron. J.* **2016**, *151*, 8. [[CrossRef](#)]
63. Knese, E.D.; Keel, W.C.; Knese, G.; Bennert, V.N.; Moiseev, A.; Grokhovskaya, A.; Dodonov, S.N. An [O III] search for extended emission around AGN with H I mapping: a distant cloud ionized by Mkn 1. *Mon. Not. R. Astron. Soc.* **2020**, *496*, 1035–1050. [[CrossRef](#)]
64. Keel, W.C.; Moiseev, A.; Kozlova, D.V.; Ikhsanova, A.I.; Oparin, D.V.; Uklein, R.I.; Smirnova, A.A.; Eselevich, M.V. The TELPERION survey for distant [O III] clouds around luminous and hibernating AGN. *Mon. Not. R. Astron. Soc.* **2022**, *510*, 4608–4625. [[CrossRef](#)]
65. Baldwin, J.A.; Phillips, M.M.; Terlevich, R. Classification parameters for the emission-line spectra of extragalactic objects. *Publ. Astron. Soc. Pac.* **1981**, *93*, 5–19. [[CrossRef](#)]
66. Groves, B.A.; Allen, M.G. ITERA: IDL tool for emission-line ratio analysis. *New Astron.* **2010**, *15*, 614–620. [[CrossRef](#)]
67. Postnikova, V.K.; Bizyaev, D. SDSS-IV MaNGA: Ionization Sources of the Extra-planar Diffuse Ionized Gas. *Astron. Lett.* **2023**, *49*, 151–166. [[CrossRef](#)]
68. Kewley, L.J.; Groves, B.; Kauffmann, G.; Heckman, T. The host galaxies and classification of active galactic nuclei. *Mon. Not. R. Astron. Soc.* **2006**, *372*, 961–976. [[CrossRef](#)]
69. Dey, A.; Schlegel, D.J.; Lang, D.; Blum, R.; Burleigh, K.; Fan, X.; Findlay, J.R.; Finkbeiner, D.; Herrera, D.; Juneau, S.; et al. Overview of the DESI Legacy Imaging Surveys. *Astron. J.* **2019**, *157*, 168. [[CrossRef](#)]
70. Keel, W.C.; Moiseev, A.; Uklein, R.I.; Smirnova, A. The TELPERION Survey for Extended Emission Regions around AGN: A strongly-interacting and merging galaxy sample. *Mon. Not. R. Astron. Soc.* **2024**, *submitted*.
71. Moran, E.C.; Halpern, J.P.; Bothun, G.D.; Becker, R.H. WAS 49: Mirror for a Hidden Seyfert 1 Nucleus. *Astron. J.* **1992**, *104*, 990. [[CrossRef](#)]
72. Merluzzi, P.; Busarello, G.; Dopita, M.A.; Thomas, A.D.; Haines, C.P.; Grado, A.; Limatola, L.; Mercurio, A. An Interacting Galaxy Pair at the Origin of a Light Echo. *Astrophys. J.* **2018**, *852*, 113. [[CrossRef](#)]
73. Moiseev, A.V.; Smirnova, A.A.; Movsessian, T.A. Enigmatic Emission Structure around Mrk 783: Cross-Ionization of a Companion 100 kpc Away. *Universe* **2023**, *9*, 493. [[CrossRef](#)]
74. Keel, W.C.; Bennert, V.N.; Pancoast, A.; Harris, C.E.; Nierenberg, A.; Chojnowski, S.D.; Moiseev, A.V.; Oparin, D.V.; Lintott, C.J.; Schawinski, K.; et al. AGN photoionization of gas in companion galaxies as a probe of AGN radiation in time and direction. *Mon. Not. R. Astron. Soc.* **2019**, *483*, 4847–4865. [[CrossRef](#)]
75. Watkins, A.E.; Mihos, J.C.; Bershady, M.; Harding, P. Discovery of a Vast Ionized Gas Cloud in the M51 System. *Astrophys. J. Lett.* **2018**, *858*, L16. [[CrossRef](#)]
76. Xu, X.; Wang, J. Ghost in the Shell: Evidence for Past Active Galactic Nucleus Activities in NGC 5195 from a Newly Discovered Large-scale Ionized Structure. *Astrophys. J.* **2023**, *943*, 28. [[CrossRef](#)]
77. Gravity Collaboration; Abuter, R.; Amorim, A.; Bauböck, M.; Berger, J.P.; Bonnet, H.; Brandner, W.; Clénet, Y.; Coudé Du Foresto, V.; de Zeeuw, P.T.; et al. A geometric distance measurement to the Galactic center black hole with 0.3% uncertainty. *Astron. Astrophys.* **2019**, *625*, L10. [[CrossRef](#)]
78. Su, M.; Slatyer, T.R.; Finkbeiner, D.P. Giant Gamma-ray Bubbles from Fermi-LAT: Active Galactic Nucleus Activity or Bipolar Galactic Wind? *Astrophys. J.* **2010**, *724*, 1044–1082. [[CrossRef](#)]
79. Barkov, M.V.; Bosch-Ramon, V. Formation of large-scale magnetic structures associated with the Fermi bubbles. *Astron. Astrophys.* **2014**, *565*, A65. [[CrossRef](#)]
80. Predehl, P.; Sunyaev, R.A.; Becker, W.; Brunner, H.; Burenin, R.; Bykov, A.; Cherepashchuk, A.; Chugai, N.; Churazov, E.; Doroshenko, V.; et al. Detection of large-scale X-ray bubbles in the Milky Way halo. *Nature* **2020**, *588*, 227–231. [[CrossRef](#)]
81. Yang, H.Y.K.; Ruszkowski, M.; Zweibel, E.G. Fermi and eROSITA bubbles as relics of the past activity of the Galaxy's central black hole. *Nat. Astron.* **2022**, *6*, 584–591. [[CrossRef](#)]
82. Bland-Hawthorn, J.; Maloney, P.R.; Sutherland, R.S.; Madsen, G.J. Fossil Imprint of a Powerful Flare at the Galactic Center along the Magellanic Stream. *Astrophys. J.* **2013**, *778*, 58. [[CrossRef](#)]
83. Bland-Hawthorn, J.; Maloney, P.R.; Sutherland, R.; Groves, B.; Guglielmo, M.; Li, W.; Curzons, A.; Cecil, G.; Fox, A.J. The Large-scale Ionization Cones in the Galaxy. *Astrophys. J.* **2019**, *886*, 45. [[CrossRef](#)]
84. Singha, M.; O'Dea, C.P.; Baum, S.A. What Drives the Ionized Gas Outflows in Radio-Quiet AGN? *Galaxies* **2023**, *11*, 85. [[CrossRef](#)]
85. Venturi, G.; Treister, E.; Finlez, C.; D'Ago, G.; Bauer, F.; Harrison, C.M.; Ramos Almeida, C.; Revalschi, M.; Ricci, F.; Sartori, L.F.; et al. Complex AGN feedback in the Teacup galaxy. A powerful ionised galactic outflow, jet-ISM interaction, and evidence for AGN-triggered star formation in a giant bubble. *Astron. Astrophys.* **2023**, *678*, A127. [[CrossRef](#)]
86. Bieri, R.; Dubois, Y.; Rosdahl, J.; Wagner, A.; Silk, J.; Mamon, G.A. Outflows driven by quasars in high-redshift galaxies with radiation hydrodynamics. *Mon. Not. R. Astron. Soc.* **2017**, *464*, 1854–1873. [[CrossRef](#)]

87. Kakiichi, K.; Graziani, L.; Ciardi, B.; Meiksin, A.; Compostella, M.; Eide, M.B.; Zaroubi, S. The concerted impact of galaxies and QSOs on the ionization and thermal state of the intergalactic medium. *Mon. Not. R. Astron. Soc.* **2017**, *468*, 3718–3736. [[CrossRef](#)]
88. Graziani, L.; Ciardi, B.; Glatzle, M. X-ray ionization of the intergalactic medium by quasars. *Mon. Not. R. Astron. Soc.* **2018**, *479*, 4320–4335. [[CrossRef](#)]
89. Cicone, C.; Maiolino, R.; Gallerani, S.; Neri, R.; Ferrara, A.; Sturm, E.; Fiore, F.; Piconcelli, E.; Feruglio, C. Very extended cold gas, star formation and outflows in the halo of a bright quasar at $z > 6$. *Astron. Astrophys.* **2015**, *574*, A14. [[CrossRef](#)]
90. Fujimoto, S.; Ouchi, M.; Ferrara, A.; Pallottini, A.; Ivison, R.J.; Behrens, C.; Gallerani, S.; Arata, S.; Yajima, H.; Nagamine, K. First Identification of 10 kpc [C II] 158 μm Halos around Star-forming Galaxies at $z = 5\text{--}7$. *Astrophys. J.* **2019**, *887*, 107. [[CrossRef](#)]
91. Pizzati, E.; Ferrara, A.; Pallottini, A.; Gallerani, S.; Vallini, L.; Decataldo, D.; Fujimoto, S. Outflows and extended [C II] haloes in high-redshift galaxies. *Mon. Not. R. Astron. Soc.* **2020**, *495*, 160–172. [[CrossRef](#)]
92. Vayner, A.; Zakamska, N.L.; Ishikawa, Y.; Sankar, S.; Wylezalek, D.; Rupke, D.S.N.; Veilleux, S.; Bertemes, C.; Barrera-Ballesteros, J.K.; Chen, H.W.; et al. First Results from the JWST Early Release Science Program Q3D: Ionization Cone, Clumpy Star Formation, and Shocks in a $z = 3$ Extremely Red Quasar Host. *Astrophys. J.* **2023**, *955*, 92. [[CrossRef](#)]
93. Veilleux, S.; Liu, W.; Vayner, A.; Wylezalek, D.; Rupke, D.S.N.; Zakamska, N.L.; Ishikawa, Y.; Bertemes, C.; Barrera-Ballesteros, J.K.; Chen, H.W.; et al. First Results from the JWST Early Release Science Program Q3D: The Warm Ionized Gas Outflow in $z 1.6$ Quasar XID 2028 and Its Impact on the Host Galaxy. *Astrophys. J.* **2023**, *953*, 56. [[CrossRef](#)]

Disclaimer/Publisher’s Note: The statements, opinions and data contained in all publications are solely those of the individual author(s) and contributor(s) and not of MDPI and/or the editor(s). MDPI and/or the editor(s) disclaim responsibility for any injury to people or property resulting from any ideas, methods, instructions or products referred to in the content.